

From Single Particle to Superfluid Excitations in a Dissipative Polariton Gas

V. Kohnle,^{1,*} Y. Léger,¹ M. Wouters,² M. Richard,³ M. T. Portella-Oberli,¹ and B. Deveaud-Plédran¹

¹*Institute of Condensed Matter Physics, École Polytechnique Fédérale de Lausanne (EPFL), CH-1015 Lausanne, Switzerland*

²*Institute of Theoretical Physics, École Polytechnique Fédérale de Lausanne, CH-1015 Lausanne, Switzerland*

³*Nano-Physics and Semiconductor group, Néel Institute, CNRS, Grenoble, France*

(Received 1 November 2010; revised manuscript received 28 April 2011; published 22 June 2011)

Using an angle-resolved heterodyne four-wave-mixing technique, we probe the low momentum excitation spectrum of a coherent polariton gas. The experimental results are well captured by the Bogoliubov transformation which describes the transition from single particle excitations of a normal fluid to soundlike excitations of a superfluid. In a dense coherent polariton gas, we find all the characteristics of a Bogoliubov transformation, i.e., the positive and negative energy branch with respect to the polariton gas energy at rest, soundlike shapes for the excitations dispersion, intensity, and linewidth ratio between the two branches in agreement with the theory. The influence of the nonequilibrium character of the polariton gas is shown by a careful analysis of its dispersion.

DOI: [10.1103/PhysRevLett.106.255302](https://doi.org/10.1103/PhysRevLett.106.255302)

PACS numbers: 67.10.-j, 71.36.+c, 78.47.nj, 78.67.De

The demonstration of superfluidity of helium II by Kapitza [1] and Allen and Misener [2] triggered fundamental theoretical research for understanding quantum fluids. London quickly linked superfluidity with Bose-Einstein condensation [3], stressing the importance of the bosonic nature of the particles. Meanwhile, Landau developed the idea of soundlike excitations of a superfluid [4]. These intuitions were later confirmed by Bogoliubov, whose microscopic theory of the weakly interacting Bose gas [5] reveals a superfluid phase in which elementary excitation is a coherent superposition of a counterpropagating particle and hole pair.

In a superfluid at equilibrium, the momentum dispersion of the excitations should deviate substantially from the parabolic single particle case. The dispersion turns linear for small wave vectors as a result of the sound-wave nature of the superfluid elementary excitations. In addition to the normal positive energy branch (NB), the Bogoliubov dispersion is expected to display a negative energy “ghost” branch (GB), resulting from the hole component of the excitation [6]. The NB and GB are the mirror image of each other and represent the dispersion of Bogoliubov excitations [7]. Superfluid excitations have been extensively investigated in both He superfluids [8–10] and ultracold atomic gases [11–13]. The first signs of a Bogoliubov transformation (BT) have been given by Vogels *et al.* [14] in atom condensates.

In a semiconductor microcavity where quantum well excitons and cavity photons are strongly coupled, light-matter quasiparticles called polaritons are formed. These composite bosons show unique properties which promote them as a model system of the weakly interacting Bose gas. Indeed, since the demonstration of Bose-Einstein condensation of polaritons [15], superfluidity of coherent polariton fluids has been assessed with the observation of zero-viscosity and critical velocity by Amo *et al.* [16]. Very recently, superfluid

excitations have been investigated through the photoluminescence of a nonresonant polariton condensate [17]. These experiments could not provide any observation of the GB though, feeding the controversy of the possibility to observe the ghost branch through photoluminescence experiments. Polariton condensation is indeed far from the theoretical case considered by Bogoliubov. A small condensate fraction [18] as well as the influence of the reservoirs of excitons [19] and opposite spin polaritons [20] can prevent the full formation of Bogoliubov excitations. Moreover, the effect of dissipation on the photoluminescence of a polariton condensate has not been investigated theoretically so far. All this could make Bogoliubov excitations very unlikely to show up in photoluminescence experiments, and other methods such as absorption, Bragg spectroscopy, or four-wave mixing (FWM) should be required to probe the ghost branch [14,21].

The peculiarity of polaritons with respect to other superfluids is their nonequilibrium nature. In the case of nonresonant excitation of the polariton condensate, the theory predicts the appearance of a flat diffusive region in the Bogoliubov dispersion around $k = 0$, resulting from the coupling between the exciton reservoir and the polariton field [7]. Under cw resonant excitation, no exciton reservoir is created, and the excitation spectrum is therefore much closer to the equilibrium Bogoliubov spectrum [22]. Under pulsed resonant excitation, however, we expect strong modifications in the polariton fluid dispersion due to the decay of the polariton population.

In the present work, following the suggestion of a recent theoretical proposal [21], we use FWM to investigate the superfluid character of a dissipative coherent polariton gas (CPG). Resonant excitation ensures that most of the injected polaritons take part in the condensed fraction, and a two-pulse sequence allows us to seed excitations within the CPG, stimulating emission from both the NB and the GB of the dispersion [Fig. 1(a)]. Our experimental access to

both these dispersions allows us to observe the modification of the polariton gas excitations and to conclude on the superfluid character of the CPG, e.g., BT. We use circularly polarized pulsed excitation and thus probe the excitations of a spin-polarized CPG in the dissipative regime. We can analyze the dynamics of the CPG excitations as the polariton density decays. We evidence the influence of dissipation on the excitation spectrum of a CPG resulting in an asymmetry of the NB and GB in the dispersion and an overestimated sound velocity.

We investigated a single 8 nm $\text{In}_{0.04}\text{Ga}_{0.96}\text{As}$ quantum well embedded in a GaAs wedge-shaped cavity [23]. The Rabi splitting is 3.4 meV at zero detuning. The sample is kept in a continuous flow cryostat at 5 K. We use a two-pulse heterodyne FWM setup. For optical excitation a 80 MHz pulsed Ti:sapphire laser is used. The 170 fs pulses (11 meV spectral width) are centered on the lower polariton (LP) $k = 0$ energy and cover the energy range of both LP and upper polariton (UP) dispersion curves. The laser beam is split in three parts: a reference, a pump (index 1), and a trigger (index 2). These last two cocircularly polarized beams are radio-frequency shifted with acousto-optic modulators by ω_1 (75 MHz) and ω_2 (79 MHz) and are focused on a 100 μm diameter spot on the sample. The pump pulse generates a CPG at rest ($k_1 = 0$). At a second time, the trigger pulse (10 times weaker) stimulates excitations in the

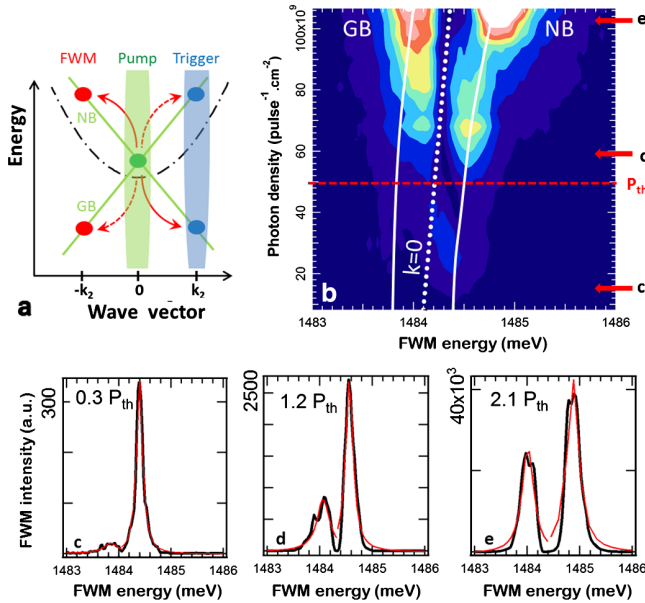


FIG. 1 (color online). (a) A femtosecond-pump pulse creates the CPG. The trigger pulse gives rise to two distinct parametric scatterings (dashed or plain red arrows). (b) FWM spectrum (linear scale) as a function of the excitation photon density. The white dashed line shows the $k = 0$ polariton energy, and the two white solid lines guide the eye and display the evolution of the NB and GB. A threshold at $P_{\text{th}} = 5 \times 10^{10}$ photons \cdot pulse $^{-1}$ cm^{-2} is observed indicated by the red dotted line. (c)–(e) show FWM spectra in the perturbative regime, slightly above threshold, and the superfluid regimes, respectively. The red curves display the Lorentz fits for the two resonances.

CPG. It carries a finite wave vector k , which is varied between $k_2 = 0$ and $1 \mu\text{m}^{-1}$. Stimulated parametric scattering of polaritons from the CPG results in the generation of a FWM signal at opposite wave vector $-k_2$. The FWM signal is selected at $k_{\text{FWM}} = 2k_1 - k_2 = -k_2$ and is directed into a mixing acousto-optic modulator together with the reference. The acousto-optic modulator, driven at $\omega_{\text{FWM}} = 2\omega_1 - \omega_2$ (71 MHz), produces two π -shifted detection channels in which the reference and FWM overlap spectrally. The mixed beams are dispersed in a spectrometer. To recover the FWM-reference interference we subtract the two π -shifted interferograms, suppressing most of the classical noise, e.g., photoluminescence. From the measured interference we retrieve the signal in amplitude and phase by spectral interferometry [24].

By using nonlinear spectroscopy, off-resonance polariton scattering has already been observed by Savvidis *et al.* [25]. However, the experiment could not allow them to demonstrate any modification of the dispersion in the vicinity of the CPG momentum. In our case, the heterodyne detection provides an experimental access to the low momentum excitations of the polariton fluid. Heterodyning allows us to separate the FWM signal from linear coherent and higher order nonlinear emission of the CPG when the standard angular selection becomes inefficient.

BT should result in a drastic change of the FWM response in terms of intensity contributions of the NB and GB modes as well as in terms of dispersion curvature. We therefore study the changes of the FWM spectrum with excitation intensity and show that the nature of the CPG excitations changes from single particles to sound waves when increasing the polariton density. Any nonlinearity in the microcavity does result in the observation of a FWM signal on the negative energy side. Here we show that this “off-resonant” emission changes drastically when the superfluid regime is reached. In this case the emission intensities of the NB and GB become comparable.

In Fig. 1(b), we plot the measured FWM spectrum as a function of excitation density at a fixed pump-trigger delay of 6.5 ps. The trigger incidence angle was kept constant to stimulate excitations at wave vector $1 \mu\text{m}^{-1}$, where the NB and GB are well separated. Two emission lines are observed. One lies below the $k = 0$ polariton energy; the other one, lying above the $k = 0$ energy, is the normal branch. At low excitation intensities (below the threshold P_{th}), the emission from the NB is much stronger than the emission of the negative energy branch [Fig. 1(c)]. Besides, the emission of the negative energy branch is symmetric to the NB emission with respect to $k = 0$. These two features demonstrate that the system is still in the perturbative regime, where the dispersion is given by the parabolic single particle one. The emission at negative energies is attributed to off-resonance polariton scattering processes. Experimentally, we observe a threshold P_{th} for the GB intensity at 5×10^{10} photons \cdot pulse $^{-1}$ cm^{-2} . Above P_{th} (dashed line), the GB emission is steeply enhanced and becomes of the same order of magnitude

as the NB emission. This shows that the excitations of the CPG have changed. Figure 1(d) shows the FWM spectrum just above P_{th} . Far above P_{th} [Fig. 1(e)], the average intensity ratio between the GB and NB is around 0.9.

The linewidth is also affected by the polariton density increase. In the low-density regime, the linewidth of the negative energy mode is much broader than the NB one. The Lorentz fits of the two resonances in Fig. 1(c) (in red) exhibit a FWHM ratio between the GB and NB of 2.6 [FWHM: 0.14 meV (0.36 meV) for the NB (GB)]. The change of the regime is accompanied by a redistribution of the linewidth. As its density increases and the ratio between the GB and NB intensity tends to one, the linewidths of the GB and NB become equal. Just above P_{th} [Fig. 1(d)], the FWHM ratio has already decreased to 1.8 [FWHM: 0.17 meV (0.30 meV) for the NB (GB)]. At high density [Fig. 1(e)], the NB and GB linewidths are 0.26 and 0.27 meV, respectively.

The relative intensities of the positive and negative energy contributions of the FWM signal can be calculated in the LP subspace, in which the polariton dynamics are described by the time-dependent Schrödinger equation:

$$i\dot{\Psi}(\vec{r}, t) = \left(\epsilon(\vec{\nabla}) + g|\Psi(\vec{r}, t)|^2 - i\frac{\gamma}{2} \right) \Psi(\vec{r}, t) + F_{p,t}(\vec{r}, t), \quad (1)$$

where Ψ is the LP wave function, ϵ its kinetic energy, g the polariton interaction constant, and $F_{p,t}$ the pump and trigger excitations. According to the design of our experiment, three modes must be considered. The CPG mode at $k = 0$ is described by φ_0 . In analogy with Bogoliubov's theory, we call u and v^* the counterpropagating perturbative modes coupled by polariton interaction. The trigger pulse excites the v^* mode, and FWM is generated on the u mode. The LP wave function reads as

$$\Psi(\vec{r}, t) = \varphi_0(\vec{r}, t) + u(\vec{r}, t)e^{i\vec{k}\vec{r}} + v^*(\vec{r}, t)e^{-i\vec{k}\vec{r}}. \quad (2)$$

Equation (1) can be solved numerically, and the spectrum of the u mode can be calculated to obtain the intensity ratio between the GB and NB. Figure 2(a) provides the calculated density evolution for the emission contribution of the NB and GB as a function of the normalized blueshift (gn_0/γ) for different excitation wave vectors. At low densities the calculated ratio is 1/3 for any wave vector. As the density increases, the elementary excitations are modified, and the u and v modes couple and redistribute polaritons in both positive and negative energy branches. The ratio tends faster to one for smaller k as expected by the equilibrium Bogoliubov theory, because for smaller k the transition is more Bogoliubov-like. The theoretical intensity ratio of 1/3 in the low-density regime comes from different damping times of the FWM resonances: It is 3 times larger for the GB resonance than for the NB resonance. This is also what we can extract from the linewidth of the emission lines as shown in Fig. 1(c). These changes in the FWM spectrum demonstrate the appearance of the Bogoliubov excitations in the CPG.

The excitation with femtosecond-laser pulses generates populations of both LPs and UPs. This yields oscillations in the excitation intensity spectrum for the NB [Fig. 1(b)]. These oscillations complicate the discussion of the NB-GB intensity ratio. They could, in principle, be avoided by shaping the excitation pulses, but this would not allow us reach the high intensities required for this experiment. The normalized NB and GB intensities are presented in Fig. 2(b) as a function of excitation intensity. The oscillation imposed by the femtosecond pulses is clearly visible [crosses in Fig. 2(b)]. In order to suppress this feature due to the LP-UP mixing, we fitted the data with a combination of an exponentially decaying sine added to a standard exponential variation [dashed lines in Fig. 2(b)]. The oscillating part is then subtracted from the data to obtain the mean GB (NB) intensity contribution [squares in Fig. 2(b)]. At low excitation power the NB emission is 4 times more intense than the GB emission. This is not far from the value of 3 expected by the perturbative theory. With increasing excitation power, the NB contribution decreases, whereas the GB contribution increases. At high excitation power, the intensities of the two branches tend to the same value as expected for the BT. The calculated density evolution for the NB and GB emission contribution [Fig. 2(a)] is displaying the experimental behavior.

To measure directly the curvatures of the NB and GB dispersion, we analyze the dependence of the FWM spectrum on the trigger wave vector. Figure 3(a) displays the spectra of the FWM signals obtained for different wave vectors of the trigger pulse integrated between 5 and 6 ps delay. The intensity of the two pulses and quite importantly of the pump pulse (12.5 mW, 10^{11} photons/pulse/cm²)

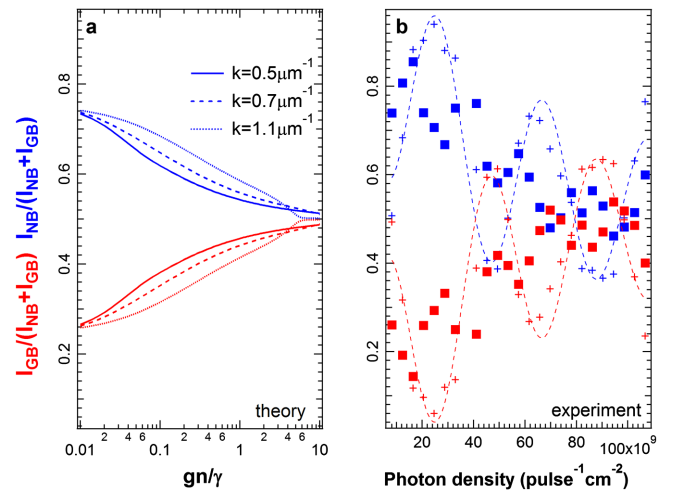


FIG. 2 (color online). (a) Calculated intensity evolution of the NB (blue) and GB (red) emission contribution plotted for different perturbation wave vectors. Calculation parameters: $\hbar\gamma = 0.1$ meV and $\hbar/2m = 0.5$ meV \cdot μm^2 . (b) Normalized intensity of the NB and GB (blue and red crosses, respectively, and dashed lines for the fits). The blue and red squares display the normalized intensities of the NB and GB with a removed oscillating part, respectively.

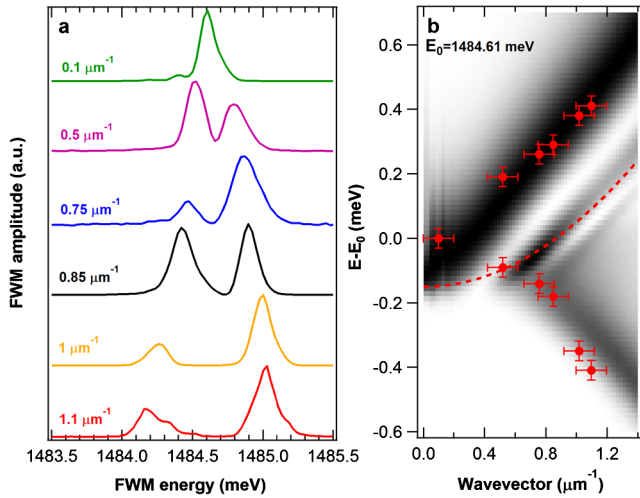


FIG. 3 (color online). (a) FWM spectra at different excitation wave vectors. (b) Energies of these lines (red dots) versus the wave vector. We compare them with the single particle parabolic dispersion (red dashed line) and with the FWM signal calculated (black) by using the Gross-Pitaevskii equations [22].

was kept constant to ensure the same polariton density in the superfluid phase for all measurements. The energies of the two emission lines are plotted in Fig. 3(b) versus the trigger wave vector. The parabolic dispersion of polaritons obtained from transmission measurements in the low-density regime is also displayed for comparison [red dashed line in Fig. 3(b)]. Theoretically, in a steady state regime the dispersion of both the NB and GB is expected to be symmetric and linear [6,22]. Indeed, the shape of the NB in our experiment is linear and strongly differs from the standard single particle parabolic dispersion. This is the consequence of polariton-polariton interactions and a clear indication of superfluidity. However, there is no symmetry between the GB and the NB at low k . Furthermore, if we extract a linear slope from the NB dispersion, we find a sound velocity $c_s = 0.6 \mu\text{m}/\text{ps}$. It does not correspond to the velocity obtained from the $k = 0$ blueshift of 0.15 meV with the equilibrium formula: $c_s = \sqrt{gn/M}$. The apparent sound velocity is thus larger than expected. This peculiar dispersion originates from the dissipative nature of polaritons. By taking the Bogoliubov equations, two physical processes can be pointed out: a blueshift of the whole dispersion corresponding to the blueshift of the condensate itself and the coupling of the two counterpropagating modes of the Bogoliubov excitations leading to the change of curvature. If the former is linear with the particle density, the latter is sublinear. The change of Bogoliubov-like curvature is therefore less sensitive to the polariton decay than dynamical blueshift. This leads to a steeper slope of the NB resulting in an apparent higher speed of sound and to the observed asymmetry in the time-integrated results. A more complete theoretical study is provided in Ref. [26]. Our calculation reproduces properly the different features of the experimental dispersion: the linearity of the NB with

an overestimated sound velocity and the asymmetry with the GB. The linearization of the Gross-Pitaevskii equation in the case of a decaying superfluid, assuming that the variations of the energies are slow, confirms the later result: The steeper slope of the NB originates from the time integration of the decaying polariton emission and not from a physical change of the sound velocity. Finally, one observes replicas of the NB at lower energy in the calculation which are also a result of the decaying superfluid density.

In conclusion, we evidenced the BT at the transition from a single particle gas to a superfluid in a semiconductor microcavity. We demonstrated the modification of the polariton dispersion curvature from parabolic in the perturbative regime to the peculiar linear dispersion of a dissipative superfluid. Despite their dissipative character, microcavity polariton gases can be qualitatively described in the frame of the Bogoliubov theory of superfluids, closely linking polariton phenomenology to cold atom physics.

We acknowledge R. Houdré and U. Oesterle for providing the sample and SNSF for financial support.

*verena.kohnle@epfl.ch

- [1] P. Kapitza, *Nature (London)* **141**, 74 (1938).
- [2] J.F. Allen and A.D. Misener, *Nature (London)* **141**, 74 (1938).
- [3] F. London, *Nature (London)* **141**, 643 (1938).
- [4] L.D. Landau, *Phys. Rev.* **60**, 356 (1941).
- [5] N.N. Bogoliubov, *J. Phys. USSR* **11**, 23 (1947).
- [6] L. Pitaevskii and S. Stringari, *Bose-Einstein Condensation* (Clarendon, Oxford, 2003), p. 56.
- [7] M. Wouters and I. Carusotto, *Phys. Rev. Lett.* **99**, 140402 (2007).
- [8] H.W. Jackson and E. Feenberg, *Rev. Mod. Phys.* **34**, 686 (1962).
- [9] A.D.B. Woods and R.A. Cowley, *Rep. Prog. Phys.* **36**, 1135 (1973).
- [10] M. Hartmann *et al.*, *Phys. Rev. Lett.* **76**, 4560 (1996).
- [11] R. Ozeri *et al.*, *Rev. Mod. Phys.* **77**, 187 (2005).
- [12] J. Steinhauer *et al.*, *Phys. Rev. Lett.* **88**, 120407 (2002).
- [13] D.S. Jin *et al.*, *Phys. Rev. Lett.* **77**, 420 (1996).
- [14] J.M. Vogels *et al.*, *Phys. Rev. Lett.* **88**, 060402 (2002).
- [15] J. Kasprzak *et al.*, *Nature (London)* **443**, 409 (2006).
- [16] A. Amo *et al.*, *Nature (London)* **457**, 291 (2009).
- [17] S. Utsunomiya *et al.*, *Nature Phys.* **4**, 700 (2008).
- [18] F.M. Marchetti *et al.*, *Phys. Rev. B* **77**, 235313 (2008).
- [19] G. Nardin *et al.*, *Phys. Rev. Lett.* **103**, 256402 (2009).
- [20] A. Shelykh *et al.*, *Phys. Status Solidi A* **202**, 2614 (2005).
- [21] M. Wouters and I. Carusotto, *Phys. Rev. B* **79**, 125311 (2009).
- [22] I. Carusotto and C. Ciuti, *Phys. Rev. Lett.* **93**, 166401 (2004).
- [23] R.P. Stanley *et al.*, *Appl. Phys. Lett.* **65**, 1883 (1994).
- [24] K.L. Hall *et al.*, *Opt. Lett.* **17**, 874 (1992).
- [25] P. Savvidis *et al.*, *Phys. Rev. B* **64**, 075311 (2001).
- [26] See supplemental material at <http://link.aps.org/supplemental/10.1103/PhysRevLett.106.255302> for the influence of dissipation.